Development 138, 4291-4299 (2011) doi:10.1242/dev.065987

Combinatorial activation and concentration-dependent repression of the *Drosophila even skipped* stripe 3+7 enhancer

Paolo Struffi*, Maria Corado, Leah Kaplan, Danyang Yu†, Christine Rushlow and Stephen Small‡

SUMMARY

Despite years of study, the precise mechanisms that control position-specific gene expression during development are not understood. Here, we analyze an enhancer element from the *even skipped* (*eve*) gene, which activates and positions two stripes of expression (stripes 3 and 7) in blastoderm stage *Drosophila* embryos. Previous genetic studies showed that the JAK-STAT pathway is required for full activation of the enhancer, whereas the gap genes *hunchback* (*hb*) and *knirps* (*kni*) are required for placement of the boundaries of both stripes. We show that the maternal zinc-finger protein Zelda (Zld) is absolutely required for activation, and present evidence that Zld binds to multiple non-canonical sites. We also use a combination of in vitro binding experiments and bioinformatics analysis to redefine the Kni-binding motif, and mutational analysis and in vivo tests to show that Kni and Hb are dedicated repressors that function by direct DNA binding. These experiments significantly extend our understanding of how the *eve* enhancer integrates positive and negative transcriptional activities to generate sharp boundaries in the early embryo.

KEY WORDS: Combinatorial control, Embryogenesis, Repression, Transcription, *Drosophila*

INTRODUCTION

Establishing temporal and spatial gene expression patterns drives the organization of complex body plans during development. At the transcriptional level, the cis-regulatory DNA elements of patterning genes integrate pre-existing asymmetric patterning information to generate expression patterns with increasingly sharp boundaries, which result in the precise placement of cells with different fates (Arnone and Davidson, 1997; Arnosti, 2003). Although hundreds of patterning elements have been discovered over the past twenty-five years, very few have been extensively studied at the molecular level.

The early *Drosophila* embryo develops as a syncytium, where positional information is in the form of transcription factor gradients. Along the anterior-posterior (AP) axis, the first gradients are maternal in origin and long-range in function, diffusing from mRNAs that are localized at or near the poles of the developing oocyte (Driever and Nusslein-Volhard, 1988; Wang and Lehmann, 1991). Maternal gradients regulate the zygotic expression of the gap genes, each of which is expressed in one or two broad domains at specific positions along the AP axis. The gap genes form gradients that act over shorter ranges and overlap at their edges, and, together with the maternal gradients, establish the seven-striped expression patterns of the pair-rule genes, including *even skipped* (*eve*) (Frasch et al., 1987; Macdonald et al., 1986). Individual *eve* stripes are controlled by modular cis-regulatory elements that respond in unique ways to the maternal and gap protein gradients (Fujioka et al., 1999; Goto et al., 1989; Harding et al., 1989; Small et al., 1992; Small et al., 1996).

The focus of this study is on a detailed characterization of a 511 bp *eve* regulatory element (*eve* 3+7) that drives strong expression of stripe 3 and much weaker expression of stripe 7 (Small et al., 1996). Genetic and mutagenesis experiments have shown that the ubiquitously activated JAK-STAT pathway is required for activation of this element (Hou et al., 1996; Yan et al., 1996), whereas the boundaries of the stripes are formed by Hunchback (Hb)- and Knirps (Kni)-mediated repression (Clyde et al., 2003; Small et al., 1996; Yu and Small, 2008). However, other mechanisms of activation must exist because mutations that remove components of the JAK-STAT pathway do not completely abolish *eve* expression. Also, although Hb and Kni are known to be crucial for forming stripe boundaries, how these proteins function at the molecular level is not clear.

Here, we describe experiments that critically test both activation and repression mechanisms. Our studies show that the ubiquitous maternal protein Zelda (Zld; Vielfaltig – FlyBase) is required for JAK-STAT-mediated activation of the *eve* 3+7 response. We also use a reiterative series of biochemical and bioinformatics analyses to redefine the DNA binding motif for Kni, and show that direct binding by Kni can account for all repressive activity on this element in the region between the two stripes. Finally, we present evidence that DNA binding sites for Hb are crucial for forming the outside boundaries of the two-stripe pattern. These results provide a firm molecular basis for understanding how repressor gradients function to differentially position multiple expression boundaries.

MATERIALS AND METHODS

Transgenes, fly stocks and embryo staining procedures

The *eve* 3+7-*lacZ* reporter was described elsewhere (Small et al., 1996). To generate the deletion mutants and all but one of the substitution mutants in the *eve* 3+7 element, site-directed mutagenesis was performed using

Department of Biology, New York University, 100 Washington Square East, New York, NY 10003, USA.

*Present address: Institute for Health and Consumer Protection, European Commission Joint Research Centre, Via Enrico Fermi 2749, 21027 Ispra (VA), Italy.
†Present address: School of Natural Sciences, Fairleigh Dickinson University, Teaneck, NJ 07666, USA.
‡Author for correspondence (sjs1@nyu.edu)

Accepted 25 July 2011

specific oligonucleotides and the Muta-Gene Phagemid Kit (Bio-Rad 170-3581). The *eve* 3+7-*lacZ* reporter containing substitution mutations in all 11 Kni binding sites (27 single-point changes in 11 sites, see Fig. 4F) was purchased from Integrated DNA Technologies (IDT). P-element-mediated transformation was used to generate transgenic lines containing all reporter constructs, and at least four independent lines were assayed by in situ hybridization with a *lacZ* probe for each construct. There was very little variation in the expression patterns between individual lines containing the same construct.

The generation of the *zld*^{294} null allele and the protocol used for obtaining germline clones in this background were described elsewhere (Liang et al., 2008).

All embryos, except those in Fig. 7, were stained using enzymatic methods (Jiang et al., 1991). Embryos in Fig. 7 were simultaneously stained for Hb and Kni proteins and *lacZ* mRNA as previously described (Wu et al., 2001).

Yeast one-hybrid analysis

To generate yeast reporters, four tandem copies of either the wild-type conserved sequence (5′-AACGCTCTACTTACCTGCAATT-3′; the sequence conserved between *D. melanogaster* and *D. picticornis* is underlined) or a mutant version (5′-AACGCTCACTAGTAGTGCAATT-3′) were cloned between the *Eco*RI and *Xba*I sites of the yeast integration and reporter vector pHISi (Matchmaker One-Hybrid System; Clontech K1603-1).

The wild-type and mutant reporters were linearized with *Xho*I and integrated into the genome of the yeast strain YM4271 (MATa, *ura3-52*, *his3-200*, *ade2-101*, *ade5*, *lys2-801*, *leu2-3*, *trp1-901*, *tyr1-501*, *gal4-Δ512*, *gal80-Δ538*, *ade5::hisG*) using the small-scale lithium acetate yeast transformation protocol (Clontech PT3024-1). 3-amino-1,2,4-triazole (3-AT) sensitivity was determined for strain YM4271[pHISi-WT] by plating 1×10^3 colonies onto SD minimal medium without histidine (Clontech 8606-1) and supplemented with 0, 1, 2.5, 5, 15, 45 or 60 mM 3-AT. Growth was completely inhibited by 5 mM 3-AT.

The wild-type reporter strain was transformed with 40 μg of a 0- to 6-hour *D. melanogaster* Oregon R poly(A)+ embryonic cDNA library constructed using the λACT phage (Yu et al., 1999) and selected in SD minimal medium with –His/–Leu dropout supplement (Clontech 8609-1) in the presence of 10 mM 3-AT, following the large-scale yeast transformation protocol (Clontech PT1031-1). The efficiency of transformation was ~4.2×10^4 transformants/μg DNA. Twenty-three clones were isolated within 5 days of transformation, from which the plasmids were recovered and sequenced. Nine clones corresponded to full-length *kni* cDNA, three clones corresponded to two different *zld* cDNAs (covering amino acids 1195-1596 and 1293-1596), whereas for the other 11 clones we found a single hit for each. Purified DNA samples from the 14 independent cDNAs were used to transform the wild-type reporter strain, but only transformants containing *kni* and *zld* cDNAs grew in the presence of 10 mM and 45 mM 3-AT (see Fig. S1 in the supplementary material). The results from this experiment suggest that the other clones were false positives. Purified plasmids from the two independent *kni* and *zld* clones were then used to transform the mutant yeast reporter strain. Both *zld* cDNA plasmids failed to activate the mutant reporter, whereas the *kni* cDNA plasmids gave transformants even in the presence of 45 mM 3-AT (see Fig. S1 in the supplementary material).

Protein expression and purification

Different *kni* fragments (see Fig. S2 in the supplementary material) were subcloned as *Kpn*I-*Xba*I inserts into a modified pGEX-6P-3 vector (Amersham Biosciences 27-4599-01). All fragments were PCR amplified from clone N741 (Nauber et al., 1988), which contains a full-length *kni* cDNA, and the final plasmids were sequenced to confirm the correct reading frame and insert integrity. The GST-ZldC expression plasmid was a gift from Nikolai Kirov (Liang et al., 2008). To generate pET-Zld, the entire *zld* coding region was PCR amplified from Canton S genomic DNA using PfuUltra II Fusion HS DNA Polymerase (Stratagene 600670) and the following primers: 5′-CGCG**GGTACC**ATGACGAGCATTAAGACC-GAGATGCC-3′ and 5′-CGCG**TCTAGA**TCAGTAGAGCTCTATGCT-CTTCTC-3′ (*Kpn*I and *Xba*I sites in bold, start and stop codons underlined). The PCR program used was: 95°C for 2 minutes; 30 cycles of 95°C for 20 seconds, 55°C for 20 seconds, 72°C for 90 seconds; followed by 72°C for 3 minutes. A 4.8 kb band was gel purified, digested with *Kpn*I and *Xba*I and ligated to a modified pET15b vector (Novagen 69661-3) restricted with *Kpn*I and *Nhe*I.

Expression plasmids were transformed into *E. coli* BL21 CodonPlus (DE3) competent cells (Stratagene 230245), and a single colony was grown in 3 ml LB Amp^{100} medium (which contains 100 μg/ml ampicillin) until early exponential phase (~5 hours). Then, 1 ml of this starter culture was expanded in 300 ml prewarmed LB Amp^{100} and grown to an OD_{600} of 0.4-0.6. Protein expression was induced by adding isopropyl-β-D-thiogalactoside to a final concentration of 0.1 mM and incubating the cultures for 3 hours at 37°C or for 6-24 hours at 18-20°C.

For the purification of GST-tagged proteins, cells were centrifuged at 7700 ***g*** for 10 minutes at 4°C and resuspended in 30 ml lysis buffer (100 mM KCl, 25 mM HEPES pH 7.9, 5 mM DTT, 20% glycerol, 1 mM benzamidine, 1 mM $Na_2S_2O_5$, 3 μM pepstatin A, 1 mM PMSF) containing 0.1 mg/ml lysozyme and kept on ice for 15 minutes. Cells were disrupted by sonication with four to six cycles of 30 seconds (50% duty cycle, output 3-4) using a Sonic Dismembrator Model 550 (Fisher Scientific) equipped with a microtip. The cell lysate was centrifuged at 4°C for 10 minutes at 12,000 ***g***, and the supernatant was transferred to a fresh tube containing 1 ml 50% slurry of glutathione Sepharose 4B beads (Amersham Biosciences 17-0756-01) prewashed in 1×PBS (140 mM NaCl, 2.7 mM KCl, 10 mM Na_2HPO_4, 1.8 mM KH_2PO_4) and pre-equilibrated in lysis buffer. Tubes were secured onto a rotator and incubated for 2 hours at 4°C with gentle agitation. Beads were sedimented by centrifugation (500 ***g***) and the supernatant was carefully discarded. Beads were then washed three times with the same volume of lysis buffer and transferred to a 2-ml microcentrifuge tube. Bound proteins were eluted from the beads by adding 1 ml elution buffer (20 mM reduced glutathione and 50 mM HEPES pH 7.9 in lysis buffer) per ml of slurry bed volume, mixing gently to resuspend the beads, and incubating for 30 minutes at 4°C with gentle rotation. Beads were sedimented and the supernatant was transferred to a fresh tube. Protein concentration was determined by the Bradford assay using BSA as a standard. For purification of GST-Kni1-429, GST-Kni1-340 and GST-Zld-C fragments, it was necessary to include detergents in order to obtain soluble proteins. For this purpose, the above protocol was integrated with one previously published (Frangioni and Neel, 1993) to include the addition of N-laurylsarkosine to a final concentration of 1.5% immediately before sonication and the addition of Triton X-100 to a final concentration of 1% after sonication. The two detergents were not included in the successive steps.

For purification of His-tagged, full-length Zld, cells were collected and sonicated as described above, but a different lysis buffer was used: 300 mM NaCl, 25 mM HEPES pH 7.9, 1 mM EDTA, 10 mM imidazole, 10% glycerol, 15 mM β-mercaptoethanol, 1 mM benzamidine, 1 mM $Na_2S_2O_5$, 10 μM pepstatin A, 1 mM PMSF. The cell lysate was centrifuged at 4°C for 10 minutes at 12,000 ***g***, and the supernatant was transferred to a fresh tube containing 0.7 ml 50% slurry of Ni-NTA agarose beads (Qiagen 30210) prewashed in 1×PBS and pre-equilibrated in lysis buffer. Incubation and washings were as described above. Bound proteins were eluted from the sedimented beads by adding 0.5 ml elution buffer (250 mM imidazole in lysis bufffer) and incubating the resuspended beads for 30 minutes at 4°C with gentle rotation. Beads were then sedimented and the supernatant transferred to a new tube.

Electrophoretic mobility shift assay (EMSA)

Oligos used for EMSA experiments were obtained from IDT (see Table S1 in the supplementary material). To generate double-stranded (ds) fragments, 7.5 μl of each complementary oligonucleotide (100 pM/μl) were combined in a 0.5 ml Eppendorf tube together with 165 μl H_2O and 20 μl annealing buffer (200 mM Tris-Cl pH 7.5, 20 mM $MgCl_2$, 500 mM NaCl). The tube was placed in a 95°C heat block, which was then cooled gradually to room temperature. Larger fragments from the *eve* 2 enhancer (see Fig. 3E,F) were generated by PCR amplification (for primers, see Table S1 in the supplementary material).

For 5′ end-labeling, 1 µl (~50 ng) dsDNA oligonucleotide was incubated for 30 minutes at 37°C with 1 µl T4 polynucleotide kinase in the presence of 1 µl [γ-^{32}P]ATP (MPI 35020), 1 µl 50 mM DDT, 1 µl 10× PNK buffer and 5 µl H_2O. To remove most of the unincorporated [γ-^{32}P]ATP, 70 µl 10 mM Tris (pH 8.0) were added to the reaction and the entire sample was loaded onto an Illustra MicroSpin G25 spin column (GE Healthcare 27-5325-01). Samples were then desiccated to a small volume (~10 µl), mixed with loading buffer and purified on a 15% native polyacrylamide gel. Bands were excised, transferred to Eppendorf tubes containing 0.5 ml elution buffer (0.5 M ammonium acetate, 10 mM magnesium acetate), and mixed for several hours at room temperature. The buffer was transferred to a low-retention tube, and DNA was precipitated in the presence of 3 µl PelletPaint co-precipitant (Novagen 69049-3), 55 µl 3 M sodium acetate (pH 5.2) and 1 ml 100% ethanol, and resuspended in 40 µl 10 mM Tris (pH 8.0). To measure the specific activity, 1 µl was transferred to a 20 ml Wheaton liquid scintillation vial (Fisher 03-341-73) containing 20 µl H_2O. Then, 10 ml liquid scintillation cocktail (MPI 882470) were added and the vial was loaded into a liquid scintillation counter (Beckman LS6000 LL). The probe was diluted to 20,000 cpm/µl using 10 mM Tris (pH 8.0).

For DNA-binding reactions, 1 µl of affinity-purified protein (0.1-2 µg) was incubated for 30 minutes at room temperature with 20 µl freshly prepared binding buffer (100 mM KCl, 10% glycerol, 20 mM HEPES pH 8.0, 1 mM DTT, 5 mM $MgCl_2$,1 µM $ZnSO_4$, 1 mM benzamidine, 1 mM $Na_2S_2O_5$, 3 µM pepstatin A, 0.1 mg/ml BSA, 1 mM PMSF), 10 mg/ml poly[d(I-C)] and 1 µl purified probe (20,000 cpm/µl). The entire binding reaction was loaded onto a pre-run 4.5% native polyacrylamide gel and run at 150 V for ~2 hours. The gel was dried and exposed to autoradiography film with an intensifying screen at –80°C for 12-16 hours.

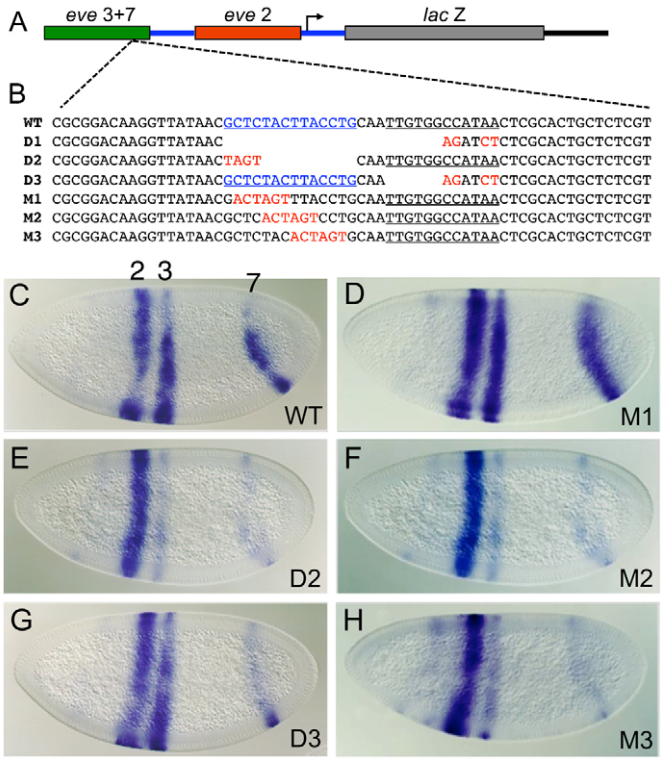

Fig. 1. Deletion and mutation analyses of two conserved regions in the *eve* 3+7 enhancer. (**A**) The reporter gene, showing the *eve* 3+7 enhancer and the *eve* 2 enhancer, separated by a 300 bp spacer sequence that ensures their autonomy (Small et al., 1993), cloned upstream of the *eve* basal promoter driving *lacZ* expression. (**B**) DNA sequence variants tested in the context of the reporter gene in A. The conserved regions between *D. melanogaster* and *D. picticornis* are underlined; three deletions (D1-D3) and three substitution mutants (M1-M3) are shown. (**C-H**) Expression of *eve* 3+7-*lacZ* reporters containing the sequence variants shown in B. Stripe numbers are shown in the wild-type (WT) panel (C). Deletion of the upstream motif (D2) caused a reduction of stripe 3 and 7 (E) similar to that observed when both motifs were deleted (D1, data not shown), whereas deletion of the downstream motif (D3) did not alter expression of stripe 3 and had a modest effect on stripe 7 (G). Mutations in the CAGGTAA site present in the reverse sequence at the 3′ end of the first motif caused reductions in the expression of both stripe 3 and 7 (F,H), whereas a mutant that does not alter this site (M1) did not cause any detectable effect on reporter gene expression (D).

RESULTS

The maternal zinc-finger protein Zelda is required for STAT-mediated activation of the *eve* 3+7 enhancer

Previous studies suggested that the JAK-STAT pathway is required for activation of the *eve* 3+7 enhancer. However, loss-of-function mutants lacking JAK-STAT components show only a partial loss of *eve* 3 expression (Hou et al., 1996; Yan et al., 1996), suggesting that other factors/pathways must be involved in enhancer activation. To identify such factors, we tested two motifs in the 3′ region of the *eve* 3+7 enhancer that are perfectly conserved between *D. melanogaster* and *D. picticornis* (Sackerson, 1995) by deleting them in the context of a reporter gene that also contained the *eve* 2 enhancer as an internal control for expression levels (Fig. 1A). Deleting both sequences (not shown) or only the upstream sequence (Fig. 1E) caused a strong reduction in expression levels of both stripe 3 and 7. By contrast, deleting the downstream motif caused a significant reduction in the stripe 7 response, but did not detectably alter the levels of stripe 3 expression (Fig. 1G).

We extended our analysis of the upstream motif by performing a linker-scanning mutagenesis experiment to identify specific base pairs required for activation of both stripes (Fig. 1B,D,F,H). These experiments identified a 9 bp region that is crucial for activation of stripes 3 and 7. Interestingly, this motif contains the sequence CAGGTAA, which is among five sequences (referred to collectively as the TAGteam DNA motif) that are over-represented in the regulatory regions of a number of early zygotically active genes (De Renzis et al., 2007; ten Bosch et al., 2006).

The ubiquitous maternal protein Zelda (Zld) binds specifically to TAGteam sites and is required for activation of a large number of genes early in development (Liang et al., 2008). The *eve* expression pattern is significantly disrupted, but not completely abolished, in embryos derived from germline clones lacking Zld (*zld* M$^-$ embryos), as compared with wild-type embryos (see Fig. S3 in the supplementary material), suggesting that other factors might bind this site. To identify such factors, we performed a yeast one-hybrid screen using a library obtained from 0- to 6-hour embryos (see Materials and methods). Out of ~1.7 million colonies screened, we identified clones for only two transcription factors: Zld and Kni (see Materials and methods and Fig. S1 in the supplementary material). We next transformed a yeast strain containing an identical reporter with substitution mutations in the 9 bp region required for enhancer activation in vivo with purified plasmids expressing these two proteins. These mutations completely prevented activation in yeast by Zld (see Fig. S1 in the supplementary material), which suggests that Zld binds specifically to the sequences required for activation of the *eve* 3+7 reporter gene. By contrast, the *kni* clones tested maintained activation of the mutated yeast construct, suggesting that any Kni-binding activity in the mutated sequence was still intact (see below).

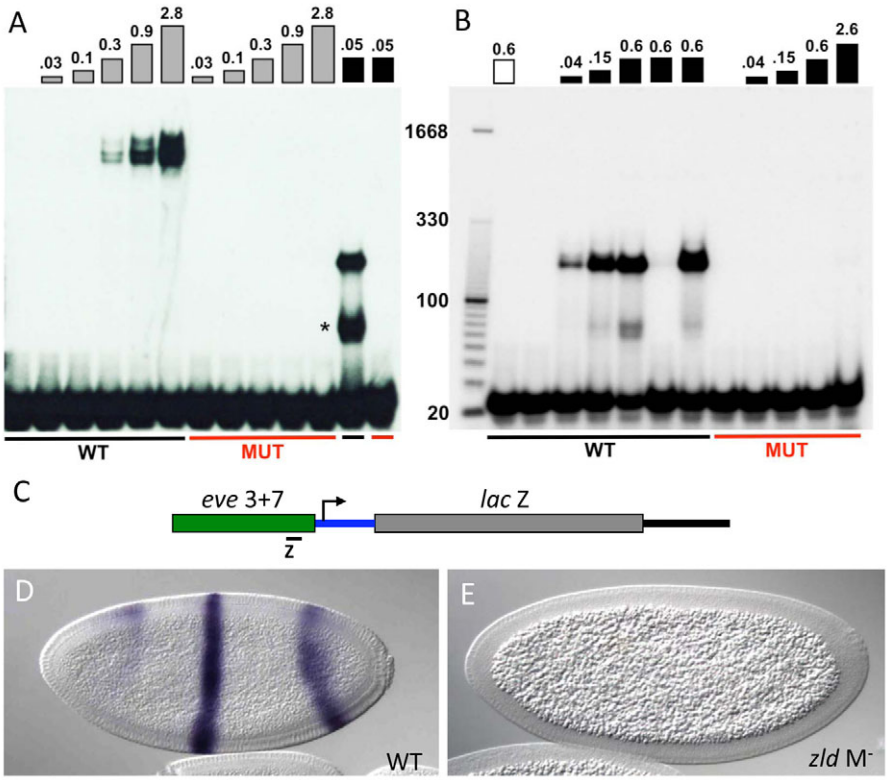

Fig. 2. Zld binds to the CAGGTAA motif and is required for activation of the *eve* 3+7 enhancer. (**A**,**B**) Electrophoretic mobility shift assays (EMSAs) using His-tagged, full-length Zld (gray), a GST fusion to a C-terminal Zld fragment (amino acids 1240-1470, GST-ZldC, black), or GST (white) are shown. Proteins were incubated with a 22 bp oligonucleotide containing the CAGGTAA sequence (WT) or a mutated version thereof (MUT; see Table S1 in the supplementary material). Numbers above the rectangles indicate the amount of protein (μg) used in each lane. The lower shifted band in the GST-ZldC lane in A (asterisk) is most likely a degradation product because it is barely detectable when using a fresh protein aliquot (B), but becomes more prominent after repeated freeze-thaw cycles. (**C**) The *eve* 3+7 reporter gene (Small et al., 1996). The position of the CAGGTAA motif (Z) is shown. (**D**,**E**) RNA expression of the *eve* 3+7-*lacZ* reporter in a wild-type *Drosophila* embryo (D) and in an embryo lacking maternal expression of Zld (*zld* M^{-}) (E).

We next examined the role of Zld in *eve* 3+7 enhancer activation. First, electrophoretic mobility shift assays (EMSAs) were performed using His-tagged, full-length Zld and GST-ZldC, which contains a cluster of four zinc-fingers near the C-terminus (Liang et al., 2008). Both proteins bound specifically to the CAGGTAA site in vitro and failed to bind to the mutated site (Fig. 2A,B). Because of the similarities in binding and technical difficulties in expressing and purifying significant amounts of soluble full-length protein, we used the truncated ZldC protein in subsequent experiments. GST-ZldC binding to the CAGGTAA site was completely abolished by competition with unlabeled wild-type oligonucleotide and was not affected by competition with the mutant oligonucleotide (Fig. 2B). We then crossed the *eve* 3+7 reporter construct into *zld* M^{-} embryos, expecting a reduction in expression levels similar to that caused by mutating the Zld site (Fig. 1). Surprisingly, expression of the wild-type construct was completely abolished in these embryos (Fig. 2E). This result indicates that Zld is absolutely required for *eve* 3+7 activation, and suggests that the JAK-STAT pathway is insufficient for enhancer activation on its own.

As a negative control, we crossed a reporter gene containing only the *eve* 2 enhancer into *zld* M^{-} embryos. This construct contains none of the previously identified TAGteam sites, but nonetheless its expression was completely abolished in embryos lacking Zld (Fig. 3C). This result, along with the stronger than expected effect on *eve* 3+7, suggest that Zld plays a more prominent role in *eve* activation than previously thought. One possibility is that these enhancers contain Zld binding sites that do not match the TAGteam sequences. Alternatively, activation by Zld might involve mechanisms that are independent of DNA binding. We tested the first hypothesis by performing EMSA on a series of four 150 bp fragments that span the *eve* 2 enhancer element as well as a 100 bp fragment containing four mutated Zld sites, which served as a negative control (Fig. 3F; data not shown). All four fragments showed some Zld-binding activity in vitro, but binding affinities to these fragments seemed somewhat lower than that of the CAGGTAA site from the *eve* 3+7 enhancer (Fig. 3F, lane 14). To identify putative Zld binding sites in the *eve* 2 element, we tested a panel of ten overlapping 21 bp probes that span fragment 4 (P32-P41). One of the probes (P41) showed clear binding (data not shown); its 5′ end includes the sequence CAGGCAA, which differs by just one nucleotide from one of the TAGteam sequences. A probe containing this site in the middle (P42) showed a similar binding activity (Fig. 3G). We then searched the *eve* 2 sequence for other variants of TAGteam motifs and identified three additional Zld sites (Fig. 3H; data not shown). These experiments suggest that activation of the *eve* 2 enhancer involves specific binding of Zld to non-canonical sites.

Kni binding is required for setting the inside boundaries of *eve* stripes 3 and 7

The abdominal Kni expression domain is positioned in the region between *eve* stripes 3 and 7, and very low levels of ectopically expressed Kni protein efficiently repress these stripes (Clyde et al., 2003; Struffi et al., 2004). In addition, the genetic removal of *kni* causes a complete derepression in this region, and DNAse I footprint assays have shown that there are at least five Kni binding sites in the minimal stripe element (Small et al., 1996).

In previous work, we attempted to mutate the footprinted Kni binding sites, but these mutations caused only minor effects on the stripe pattern (data not shown). These results suggest that either the tested mutations did not remove all Kni-binding activity or that Kni-mediated repression is indirect. To identify additional sites, we used a position weight matrix (PWM) derived from seventeen footprinted Kni sites in the literature (Fig. 4B) (Lifanov et al., 2003). This PWM predicted 12 Kni sites in the minimal enhancer,

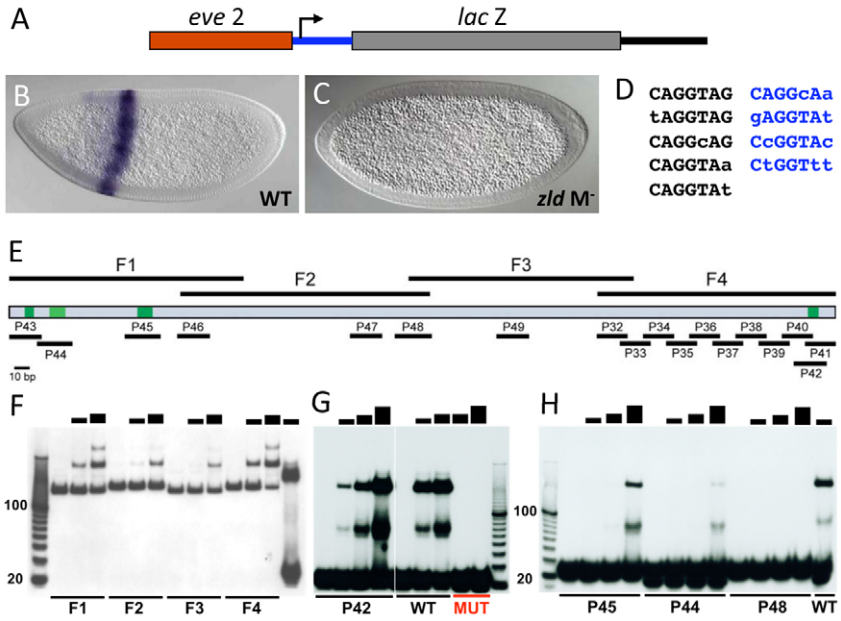

Fig. 3. Zld is required for activation of the *eve* stripe 2 enhancer and binds to non-canonical TAGteam sites. (**A**) The *eve* 2-*lacZ* reporter gene (Small et al., 1992). (**B**,**C**) RNA expression of the *eve* 2-*lacZ* reporter in a wild-type *Drosophila* embryo (B) and in a *zld* M⁻ embryo (C). (**D**) A summary of verified Zld binding sites. Canonical sites (black) and new sites discovered here (blue) are shown. (**E**) The *eve* 2 element, showing the positions of non-canonical Zld binding sites (green boxes). PCR fragments (F1-4) and oligonucleotide probes (P32-49) used for EMSA experiments (in F-H) are indicated. (**F-H**) EMSA experiments using affinity-purified GST-ZldC. Lanes are labeled according to the schematic in E. Boxes above the lanes indicate the amount of GST-ZldC used in each reaction: small box, 50 ng; medium, 200 ng; tall, 800 ng.

and substitution mutations in the core motifs of six of these sites led to a modest posterior expansion of the stripe into the region between stripes 3 and 4 (Clyde et al., 2003). However, subsequent attempts to completely remove Kni-binding activity caused no further expansions (data not shown). A possible explanation for these results is that the predicted sites do not reflect the true binding capabilities of Kni. Therefore, we tested the predicted sites one by one in gel shift experiments using an affinity-purified Kni protein fragment containing its DNA-binding domain and nuclear localization signal fused to GST (GST-Kni1-105). In 8 of 12 cases, the predicted sites did not show strong binding and in some cases the PWM score did not correlate with the binding affinity observed (data not shown). Also, the conserved binding motif adjacent to the Zld site seemed to bind strongly to Kni in the one-hybrid experiment (see Fig. S1 in the supplementary material), but was not predicted by the PWM. This Kni site was tested directly and found to bind specifically in EMSA experiments (P25, Fig. 5). The poor match between predicted and confirmed Kni sites prompted us to scan the entire *eve* 3+7 element for more binding sites using overlapping oligonucleotides (Fig. 4A). These experiments identified 11 fragments of various lengths, each of which exhibited Kni-binding activity (Fig. 5), but it was not possible to align common sequence motifs among these fragments.

We then obtained a different PWM derived from a single SELEX experiment performed by the Berkeley Drosophila Transcription Network Project (Fig. 4C). Despite the low specificity of this PWM, it predicted twenty sites in the *eve* 3+7 enhancer. Strikingly, 11 of the predicted sites mapped to each of the 11 Kni-binding fragments identified in vitro, whereas the other nine mapped to regions that did not bind. By considering only those predicted sites that bound, we generated a more specific PWM (Fig. 4D), which was substantially different from that predicted from footprinted sites in the literature (Fig. 4B). Interestingly, Noyes et al. (Noyes et al., 2008) published a new PWM for Kni based on data from a bacterial one-hybrid experiment (Fig. 4E), and this is remarkably similar to that derived from our direct Kni binding studies. The similar PWMs showed three bases (positions 1, 6 and 9) that are nearly invariant. Changing two or three of these bases completely abolished binding to nine of the 11 sites (Fig. 5), suggesting that these PWMs accurately identify bases required for effective Kni binding. We introduced mutations into each of the 11 predicted sites (Fig. 4F) in the context of an *eve* 3+7-*lacZ* transgene and tested its activity in vivo. These mutations converted the striped, wild-type pattern (Fig. 4G) into a single broad expression domain in the posterior part of the embryo (Fig. 4H). This pattern is virtually indistinguishable from that driven by the wild-type enhancer in *kni* mutants, suggesting that the invariant bases in the predicted Kni sites are crucial for Kni activity in vivo.

Hb binding is required for positioning the outside boundaries of *eve* stripes 3 and 7

The gap protein Hb is expressed maternally and zygotically in a dynamic pattern that includes expression throughout the anterior half of the embryo and a broad stripe in posterior regions (Tautz et al., 1987). Previous studies suggested that Hb acts as a repressor that forms the anterior boundary of *eve* stripe 3 and the posterior boundary of stripe 7 (Clyde et al., 2003; Small et al., 1996; Yu and Small, 2008). Misexpression of Hb causes a dose-dependent reduction of these stripes, and there are numerous Hb binding sites in the *eve* 3+7 element (Stanojevic et al., 1989). However, recent computational work suggests that Hb might act in both the activation and repression of the stripe (Papatsenko and Levine, 2008). According to this model, high levels of Hb repress expression, whereas lower levels are involved in activation. This is consistent with a similar model for Hb-mediated regulation of the gap gene *Krüppel* (*Kr*), which is expressed in a central domain (Schulz and Tautz, 1994).

A computational scan of the *eve* 3+7 enhancer predicts nine Hb binding sites with relatively high PWM scores (Fig. 6A) (Lifanov et al., 2003). There is excellent agreement between the positions of these sites and previous footprint studies of Hb binding to the *eve* promoter region (Stanojevic et al., 1989). To test the role of Hb in *eve* 3+7 regulation, we generated specific substitution mutations in predicted Hb binding sites and then tested them in reporter gene assays in vivo (Fig. 6). Mutations in four predicted sites led to an anterior derepression of stripe 3 expression and to a strengthening and posterior expansion of stripe 7 (Fig. 6C), results which are qualitatively similar to the expansions observed in *hb* mutants

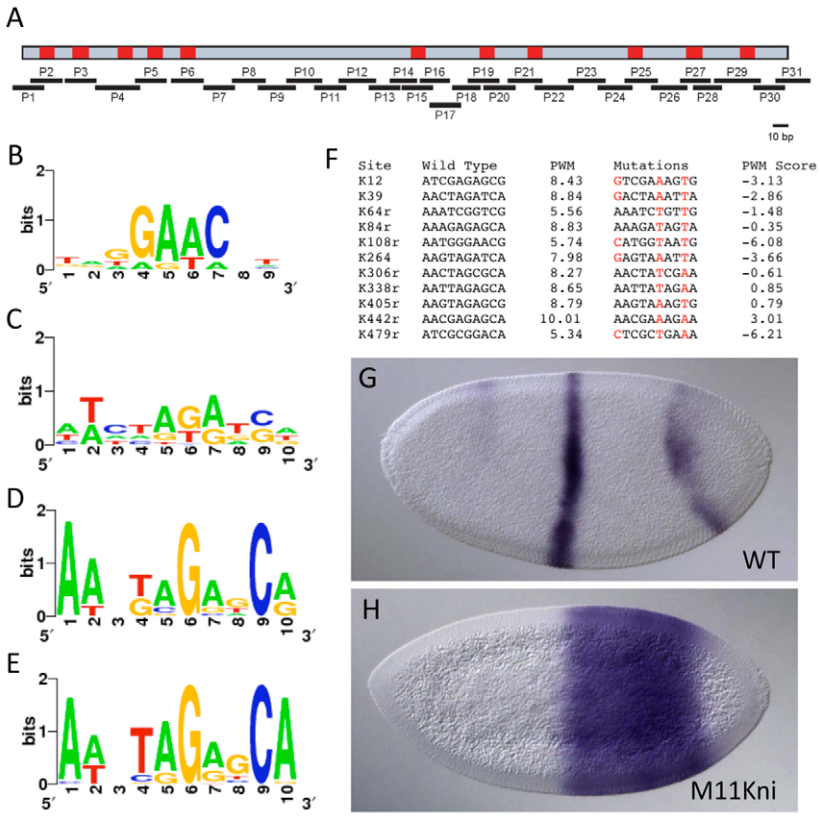

Fig. 4. Kni represses the *eve* 3+7 enhancer through direct binding to 11 sites. (**A**) The 511 bp *eve* 3+7 enhancer (gray bar) showing the positions of DNA probes (P1-P31) used in gel shift assays. Kni sites identified in the EMSA experiments shown in Fig. 5 are indicated as red boxes. (**B-E**) Position weight matrices (PWMs) derived from various collections of Kni binding site datasets (see text). (**F**) Sequences of Kni binding sites in the *eve* 3+7 enhancer (left), and point mutations of those sites that were tested in vivo (right). Sites are numbered by their position in the 511 bp enhancer; reverse strand sites are indicated (r). PWM scores are shown for wild-type sites and their mutated counterparts. (**G**,**H**) *lacZ* expression patterns driven by the wild-type *eve* 3+7 reporter gene (G) and an identical reporter that contains mutations in all 11 Kni binding sites (H). Such mutations cause complete derepression in the region between the stripes.

(Small et al., 1996). This is consistent with the hypothesis that high levels of Hb are required for effective repression of the enhancer (Clyde et al., 2003; Yu and Small, 2008). We next made mutations in all nine predicted Hb sites in an effort to completely abolish all Hb-binding activity from the enhancer (M9 Hb, Fig. 6A). If Hb is involved in both repression and activation, the complete removal of Hb binding might be expected to cause a reduction in stripe levels. Instead, this construct caused expansions that were very similar to those observed after mutating four sites (Fig. 6D).

DISCUSSION

The experiments described here significantly refine our understanding of how the *eve* 3+7 enhancer functions in the early embryo. In particular, we showed that the maternal zinc-finger protein Zld is absolutely required for STAT-mediated enhancer activation, and that the gap proteins Kni and Hb establish stripe boundaries by directly binding to multiple sites within the enhancer (Fig. 7A,B; see Fig. S4 in the supplementary material).

The mechanism of enhancer activation

When first activated in late nuclear cycle 13, the minimal *eve* 3+7 enhancer drives weak stochastic expression in a broad central pattern (Fig. 7C), which refines in cycle 14 to a stripe that is about four nuclei wide (Fig. 7D). By contrast, stripe 7 expression, which is visible by enzymatic staining methods (Fig. 1C-H, Fig. 2D, Fig. 4G), is nearly undetectable using fluorescence in situ hybridization. Previous work showed that stripe 7 shares regulatory information with stripe 3 but is also controlled by sequences located between the minimal stripe 3+7 and stripe 2 enhancers (Small et al., 1996), and possibly by sequences within and downstream of the stripe 2 enhancer (Janssens et al., 2006). Thus, stripe 7 is unique among the *eve* stripes in that it is not regulated by a discrete modular element. Previous work showed that the terminal gap gene *tailless* (*tll*) is required for activation of *eve* 7. However, since the Tll protein probably functions as a dedicated repressor (Haecker et al., 2007), it is likely that activation of *eve* 7 by Tll occurs indirectly, through repression of one or more repressors (Janssens et al., 2006).

The ubiquitous maternal protein Zld is required for the in vivo function of both the *eve* 3+7 and *eve* 2 enhancers, which are activated by the JAK-STAT pathway and Bicoid (Bcd), respectively. Zld was previously shown to bind to five sequence motifs (TAGteam sites) that are over-represented in the regulatory regions of early developmental genes (De Renzis et al., 2007; ten Bosch et al., 2006). Our mutations of the single TAGteam site in the *eve* 3+7 enhancer caused a reduction in expression (Fig. 1F,H), but *zld* M$^-$ embryos showed complete abolishment of *eve* 3+7-*lacZ* reporter gene expression (Fig. 2E). Also, the *eve* 2 enhancer, which does not contain any canonical TAGteam sites, is nonetheless inactive in *zld* M$^-$ embryos (Fig. 3C). We show here that this enhancer contains at least four variants of the TAGteam sites (Fig. 3D), which suggests that Zld binding to non-canonical sites is crucial for its function in embryogenesis. ChIP-Chip data show that Zld binding extends throughout much of the *eve* 5′ and 3′ regulatory regions (C. Nien, H. Liang and C.R., unpublished).

The implication of such broad binding and the requirement for Zld for activation of two *eve* enhancers are consistent with its proposed role as a global activator of zygotic transcription (Liang et al., 2008). How might this work? One possibility is that there are cooperative interactions between Zld and the other activators of these stripes. A non-exclusive alternative is that Zld binding creates a permissive environment in broad regions of the genome, possibly by changing the chromatin configuration and making it more likely that the other activator proteins can bind. However, it is important to note that *eve* expression is not completely abolished in *zld* M$^-$

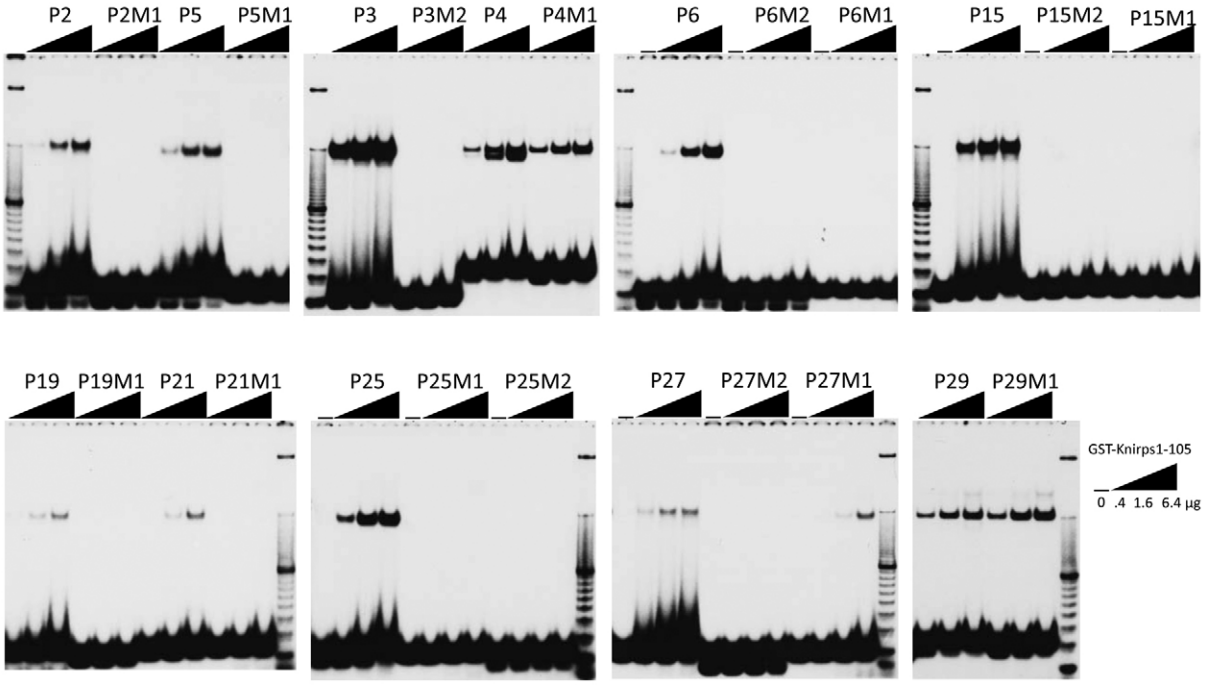

Fig. 5. Mutational analysis of Kni binding in the *eve* 3+7 enhancer. Data are shown for wild-type probes that exhibit Kni-binding activity (P2, P5, etc.), which are labeled as in Fig. 4A. For sequences of all probes and mutated versions, see Table S1 in the supplementary material. Note that different sites bind GST-Kni1-105 with very different apparent affinities (e.g. compare P3 with P19). For each site, two or three nucleotides were mutated (e.g. P25M1, P5M1) and were tested in parallel with the wild type. Such mutations effectively abolished binding in all but two cases (P4 and P29) (see text).

embryos, so at least some *eve* regulatory elements could function in the absence of Zld. Future experiments will be required to further characterize the role of Zld in the regulation of the entire *eve* locus.

Mechanisms of repression of the *eve* 3+7 enhancer

The genetic removal of *kni* causes a broad expansion of *eve* 3+7-*lacZ* expression in posterior regions of the embryo (Small et al., 1996), and ectopic Kni causes a strong repression of both stripes (Clyde et al., 2003; Struffi et al., 2004). Interestingly, the posterior boundary of *eve* stripe 3 is positioned in regions with extremely low levels of Kni protein (Fig. 7D). If the stripe 3 posterior boundary is solely formed by Kni, the enhancer must be exquisitely sensitive to its repression, possibly through the high number of sites in the *eve* 3+7 enhancer. Previous attempts to mutate sites based on computational predictions failed to mimic the genetic loss of *kni*, so here we used a biochemical approach to identify Kni sites in an unbiased manner. Our EMSA analyses identified 11 Kni sites, and the PWM derived from these sites alone is very similar to the Kni matrix derived in a bacterial one-hybrid study (Noyes et al., 2008). Thus, our studies provide biochemical support for the bacterial one-hybrid method as an accurate predictor of the DNA-binding activity of this particular protein.

We further showed that specific point mutations abolish binding to nine of the 11 sites, and when these mutations were tested in a reporter gene they caused an expansion that is indistinguishable from that detected in *kni* mutants (Small et al., 1996). This result strongly suggests that Kni-mediated repression involves direct binding to the *eve* 3+7 enhancer, and that Kni alone can account for all repressive activity in nuclei that lie in the region between stripes 3 and 7. However, our work does not address the exact mechanism of Kni-mediated repression. The simplest possibility is that Kni competes with activator proteins for binding to overlapping or adjacent sites (Levine and Manley, 1989). We consider this mechanism unlikely because only one of the 11 Kni sites overlaps with an activator site. Also, the in vivo misexpression of a truncated Kni protein (Kni 1-105) that contains only the DNA-binding domain and the nuclear localization signal has no discernible effect on the endogenous *eve* expression pattern, whereas a similar misexpression of Kni 1-330 or Kni 1-429 strongly represses *eve* 3+7 (P. Struffi, PhD thesis, Michigan State University, 2004) (Struffi et al., 2004).

Whereas Kni-mediated repression forms the inside boundaries of the *eve* 3+7 pattern, forming the outside boundaries is dependent on Hb, which abuts the anterior boundary of stripe 3 and overlaps with stripe 7 (Fig. 7D). Both stripes expand towards the poles of the embryo in zygotic *hb* mutants (Small et al., 1996), and these expansions are mimicked by mutations in four or all nine Hb sites within the *eve* 3+7 enhancer (Fig. 6C,D). Further anterior expansions of the pattern are prevented by an unknown Bcd-dependent repressor (X) and the Torso (Tor)-dependent terminal system (Fig. 7A). Indeed, *eve* 3+7-*lacZ* expression expands all the way to the anterior tip in mutants that remove *bcd* and the terminal system (Small et al., 1996).

Our mutational analyses suggest that Hb is a dedicated repressor of the *eve* 3+7 enhancer, and argue against a dual role in which high Hb levels repress, whereas lower concentrations activate, transcription (Papatsenko and Levine, 2008). One caveat is that activation of the stripe might occur via maternal

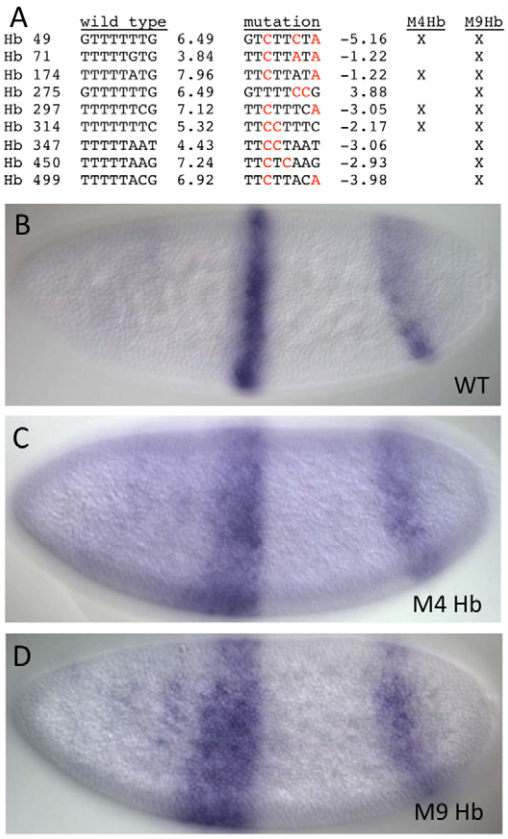

Fig. 6. Hb represses the *eve* 3+7 enhancer through direct binding to nine sites. (**A**) Sequences of Hb binding sites in the *eve* 3+7 enhancer (wild type) and point mutations (red letters) of those sites that were tested in vivo. Sites are numbered by their position in the 511 bp enhancer; reverse strand sites are indicated (r). The Hb PWM was based on published binding sites (Lifanov et al., 2003). Scores are shown for wild-type sites and their mutated counterparts, and sites mutated in individual reporter genes are indicated on the right. (**B-D**) *lacZ* expression patterns driven by the wild-type *eve* 3+7 reporter gene (B) and an identical reporter that contains mutations in four (C) or nine (D) binding sites. Mutations in Hb sites cause anterior expansions of stripe 3 expression.

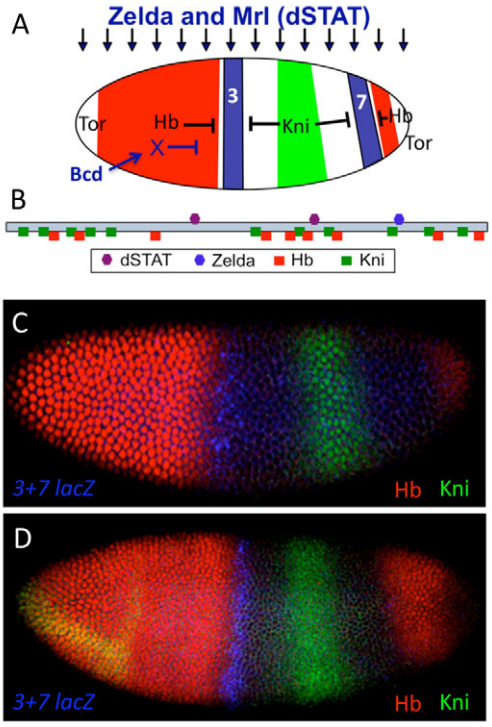

Fig. 7. Combinatorial activation and repression of the *Drosophila eve* 3+7 enhancer. (**A**) Model for the regulatory interactions that establish *eve* stripe 3 and 7 expression. Ubiquitous activators are shown as downward facing arrows along the length of the embryo, whereas the positions of the stripes are shown along with the repressive factors that prevent their activation in various regions of the embryo. (**B**) Schematic of the 511 bp enhancer showing relative positions of all verified binding sites. 'X' refers to an unknown Bcd-dependent repressor. dSTAT is also known as Mrl or Stat92E. (**C**,**D**) RNA expression of the *eve* 3+7-*lacZ* reporter gene (blue) along with Hb (red) and Kni (green) protein expression patterns in a late cycle 13 embryo (C) and an early nuclear cycle 14 embryo (D). Note that the early expression of stripe 3 is broad, but then refines to a narrow stripe. The stripe 7 response driven by the minimal element used here is always weak compared with stripe 3 and is not visible in these embryos.

Hb in the absence of zygotic expression. However, triple mutants that remove zygotic *hb*, *kni* and *tor*, a terminal system component, show *eve* 3+7 enhancer expression that extends from ~75% embryo length (100% is the anterior pole) to the posterior pole (Small et al., 1996). It is extremely unlikely that the maternal Hb gradient, which is not perturbed in this mutant combination, could activate expression throughout the posterior region. We propose that any activating role for Hb on this enhancer is indirect and might occur by repressing *kni*, which helps to define a space where the concentrations of both repressors are sufficiently low for activation to occur. *kni* expands anteriorly in *hb* mutants and is very sensitive to repression by ectopic Hb (Clyde et al., 2003; Yu and Small, 2008), consistent with an indirect role in activation. A similar mechanism has been shown to be important for the correct positioning of *eve* stripe 2 (Wu et al., 1998). In this case, the anterior Giant (Gt) domain appears to be required for *eve* 2 activation, but it does so by strongly repressing *Kr*, thus creating space for activation in the region between Gt and Kr.

The correct ordering of gene expression boundaries along the AP axis is crucial for establishing the *Drosophila* body plan. All gap genes analyzed so far seem to function as repressors that differentially position multiple boundaries (Andrioli et al., 2004; Clyde et al., 2003; Langeland et al., 1994; Struffi et al., 2004; Wu et al., 1998; Yu and Small, 2008). However, it is still unclear how differential sensitivity is achieved at the molecular level. Simple correlations of binding site number and affinity with boundary positioning cannot explain the exquisite differences in the sensitivity of individual enhancers, suggesting that they do more than 'count' binding sites and that specific arrangements of repressor and activator sites might control this process. The experiments described here better define the binding characteristics of both Hb and Kni and provide a firm foundation for future experiments designed to decipher the regulatory logic that controls differential sensitivity.

Acknowledgements
We thank Vikram Vasisht, Arthi Palaniappan, Zhe Xu, Cristina Pomilla, Hsuan-Ni Lin and Adam Parè for technical assistance; Hsiao-lan Liang for the *zld*^{294} allele; Nikolai Kirov and Tenzin Gocha for GST-ZldC; Nobuo Ogawa and Mark

Biggin for the PWM used to align Kni binding sites; Leslie Pick for the *Drosophila* embryonic cDNA library; and Hongtao Chen and Jerry Huang for comments on the manuscript. We also thank three anonymous reviewers for suggestions that improved the manuscript.

Funding
This work was supported by NIH grants RO1 GM51946 and RO1 GM63024 to S.S. and C.R., respectively, and was conducted in a facility constructed with support from Research Facilities Improvement Grant C06 RR-15518-01 from the National Center for Research Resources, National Institutes of Health. Deposited in PMC for release after 12 months.

Competing interests statement
The authors declare no competing financial interests.

Supplementary material
Supplementary material for this article is available at
http://dev.biologists.org/lookup/suppl/doi:10.1242/dev.065987/-/DC1

References

Andrioli, L. P., Oberstein, A. L., Corado, M. S., Yu, D. and Small, S. (2004). Groucho-dependent repression by Sloppy-paired 1 differentially positions anterior pair-rule stripes in the *Drosophila* embryo. *Dev. Biol.* **276**, 541-551.

Arnone, M. I. and Davidson, E. H. (1997). The hardwiring of development: organization and function of genomic regulatory systems. *Development* **124**, 1851-1864.

Arnosti, D. N. (2003). Analysis and function of transcriptional regulatory elements: insights from *Drosophila*. *Annu. Rev. Entomol.* **48**, 579-602.

Clyde, D. E., Corado, M. S., Wu, X., Pare, A., Papatsenko, D. and Small, S. (2003). A self-organizing system of repressor gradients establishes segmental complexity in *Drosophila*. *Nature* **426**, 849-853.

De Renzis, S., Elemento, O., Tavazoie, S. and Wieschaus, E. F. (2007). Unmasking activation of the zygotic genome using chromosomal deletions in the *Drosophila* embryo. *PLoS Biol.* **5**, e117.

Driever, W. and Nusslein-Volhard, C. (1988). A gradient of bicoid protein in *Drosophila* embryos. *Cell* **54**, 83-93.

Frangioni, J. V. and Neel, B. G. (1993). Solubilization and purification of enzymatically active glutathione S-transferase (pGEX) fusion proteins. *Anal. Biochem.* **210**, 179-187.

Frasch, M., Hoey, T., Rushlow, C., Doyle, H. and Levine, M. (1987). Characterization and localization of the even-skipped protein of *Drosophila*. *EMBO J.* **6**, 749-759.

Fujioka, M., Emi-Sarker, Y., Yusibova, G. L., Goto, T. and Jaynes, J. B. (1999). Analysis of an even-skipped rescue transgene reveals both composite and discrete neuronal and early blastoderm enhancers, and multi-stripe positioning by gap gene repressor gradients. *Development* **126**, 2527-2538.

Goto, T., Macdonald, P. and Maniatis, T. (1989). Early and late periodic patterns of even skipped expression are controlled by distinct regulatory elements that respond to different spatial cues. *Cell* **57**, 413-422.

Haecker, A., Qi, D., Lilja, T., Moussian, B., Andrioli, L. P., Luschnig, S. and Mannervik, M. (2007). *Drosophila* brakeless interacts with atrophin and is required for tailless-mediated transcriptional repression in early embryos. *PLoS Biol.* **5**, e145.

Harding, K., Hoey, T., Warrior, R. and Levine, M. (1989). Autoregulatory and gap gene response elements of the even-skipped promoter of *Drosophila*. *EMBO J.* **8**, 1205-1212.

Hou, X. S., Melnick, M. B. and Perrimon, N. (1996). Marelle acts downstream of the *Drosophila* HOP/JAK kinase and encodes a protein similar to the mammalian STATs. *Cell* **84**, 411-419.

Janssens, H., Hou, S., Jaeger, J., Kim, A. R., Myasnikova, E., Sharp, D. and Reinitz, J. (2006). Quantitative and predictive model of transcriptional control of the *Drosophila melanogaster* even skipped gene. *Nat. Genet.* **38**, 1159-1165.

Jiang, J., Kosman, D., Ip, Y. T. and Levine, M. (1991). The dorsal morphogen gradient regulates the mesoderm determinant twist in early *Drosophila* embryos. *Genes Dev.* **5**, 1881-1891.

Langeland, J. A., Attai, S. F., Vorwerk, K. and Carroll, S. B. (1994). Positioning adjacent pair-rule stripes in the posterior *Drosophila* embryo. *Development* **120**, 2945-2955.

Levine, M. and Manley, J. L. (1989). Transcriptional repression of eukaryotic promoters. *Cell* **59**, 405-408.

Liang, H. L., Nien, C. Y., Liu, H. Y., Metzstein, M. M., Kirov, N. and Rushlow, C. (2008). The zinc-finger protein Zelda is a key activator of the early zygotic genome in *Drosophila*. *Nature* **456**, 400-403.

Lifanov, A. P., Makeev, V. J., Nazina, A. G. and Papatsenko, D. A. (2003). Homotypic regulatory clusters in *Drosophila*. *Genome Res.* **13**, 579-588.

Macdonald, P. M., Ingham, P. and Struhl, G. (1986). Isolation, structure, and expression of even-skipped: a second pair- rule gene of *Drosophila* containing a homeo box. *Cell* **47**, 721-734.

Nauber, U., Pankratz, M. J., Kienlin, A., Seifert, E., Klemm, U. and Jackle, H. (1988). Abdominal segmentation of the *Drosophila* embryo requires a hormone receptor-like protein encoded by the gap gene knirps. *Nature* **336**, 489-492.

Noyes, M. B., Meng, X., Wakabayashi, A., Sinha, S., Brodsky, M. H. and Wolfe, S. A. (2008). A systematic characterization of factors that regulate *Drosophila* segmentation via a bacterial one-hybrid system. *Nucleic Acids Res.* **36**, 2547-2560.

Papatsenko, D. and Levine, M. S. (2008). Dual regulation by the Hunchback gradient in the *Drosophila* embryo. *Proc. Natl. Acad. Sci. USA* **105**, 2901-2906.

Sackerson, C. (1995). Patterns of conservation and divergence at the even-skipped locus of *Drosophila*. *Mech. Dev.* **51**, 199-215.

Schulz, C. and Tautz, D. (1994). Autonomous concentration-dependent activation and repression of Kruppel by hunchback in the *Drosophila* embryo. *Development* **120**, 3043-3049.

Small, S., Blair, A. and Levine, M. (1992). Regulation of even-skipped stripe 2 in the *Drosophila* embryo. *EMBO J.* **11**, 4047-4057.

Small, S., Arnosti, D. N. and Levine, M. (1993). Spacing ensures autonomous expression of different stripe enhancers in the even-skipped promoter. *Development* **119**, 762-772.

Small, S., Blair, A. and Levine, M. (1996). Regulation of two pair-rule stripes by a single enhancer in the *Drosophila* embryo. *Dev. Biol.* **175**, 314-324.

Stanojevic, D., Hoey, T. and Levine, M. (1989). Sequence-specific DNA-binding activities of the gap proteins encoded by hunchback and Kruppel in *Drosophila*. *Nature* **341**, 331-335.

Struffi, P., Corado, M., Kulkarni, M. and Arnosti, D. N. (2004). Quantitative contributions of CtBP-dependent and -independent repression activities of Knirps. *Development* **131**, 2419-2429.

Tautz, D., Lehmann, R., Schnurch, H., Schuh, R., Seifert, E., Kienlin, A., Jones, K. and Jackle, H. (1987). Finger protein of novel structure encoded by hunchback, a second member of the gap class of *Drosophila* segmentation genes. *Nature* **327**, 383-389.

ten Bosch, J. R., Benavides, J. A. and Cline, T. W. (2006). The TAGteam DNA motif controls the timing of *Drosophila* pre-blastoderm transcription. *Development* **133**, 1967-1977.

Wang, C. and Lehmann, R. (1991). Nanos is the localized posterior determinant in *Drosophila*. *Cell* **66**, 637-647.

Wu, X., Vakani, R. and Small, S. (1998). Two distinct mechanisms for differential positioning of gene expression borders involving the *Drosophila* gap protein giant. *Development* **125**, 3765-3774.

Wu, X., Vasisht, V., Kosman, D., Reinitz, J. and Small, S. (2001). Thoracic patterning by the *Drosophila* gap gene hunchback. *Dev. Biol.* **237**, 79-92.

Yan, R., Small, S., Desplan, C., Dearolf, C. R. and Darnell, J. E., Jr (1996). Identification of a Stat gene that functions in *Drosophila* development. *Cell* **84**, 421-430.

Yu, D. and Small, S. (2008). Precise registration of gene expression boundaries by a repressive morphogen in *Drosophila*. *Curr. Biol.* **18**, 868-876.

Yu, Y., Yussa, M., Song, J., Hirsch, J. and Pick, L. (1999). A double interaction screen identifies positive and negative ftz gene regulators and ftz-interacting proteins. *Mech. Dev.* **83**, 95-105.

A

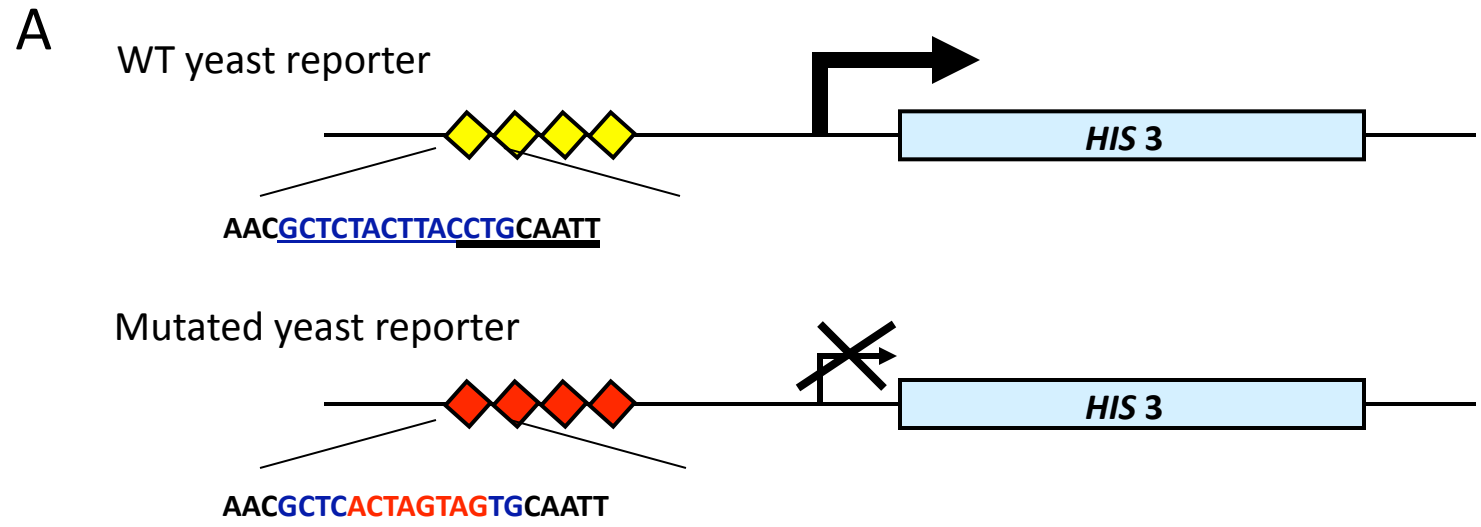

B

[3-AT]	Clone #	Gene	WT reporter 0	WT reporter 10mM	WT reporter 45mM	Mut reporter 0	Mut reporter 10mM	Mut reporter 45mM
	1,**2**,3,**4**,5, 6,7,17,18	*kni*	$3.1X10^3$	$1.6X10^3$	$1.2X10^3$	$3.0X10^3$	$2X10^3$	$0.3X10^3$
	8,**10**,18	*Zld*	$3.8X10^3$	$1.5X10^3$	$0.5X10^3$	$3.0X10^3$	0	0

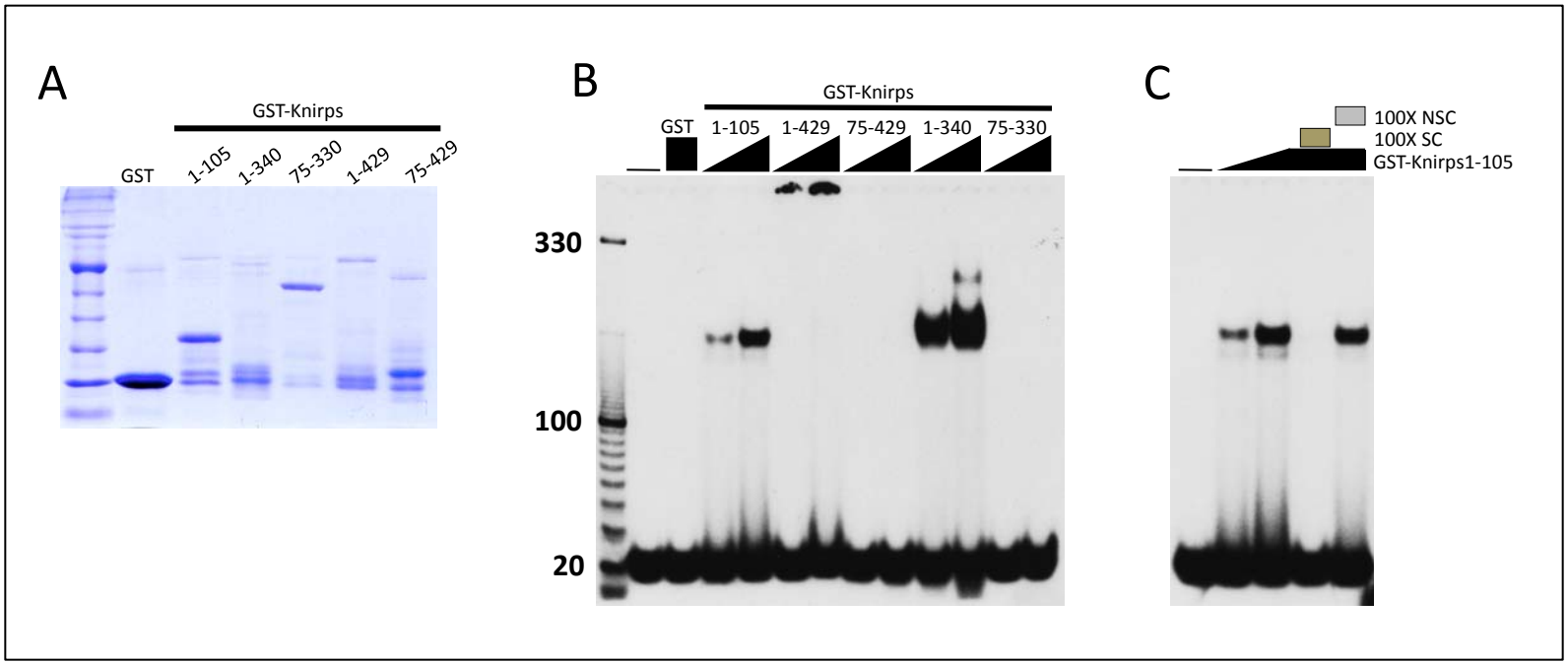
A
GST-Knirps
GST
1-105
1-340
75-330
1-429
75-429
B
GST-Knirps
GST
1-105
1-429
75-429
1-340
75-330
330
100
20
C
100X NSC
100X SC
GST-Knirps1-105

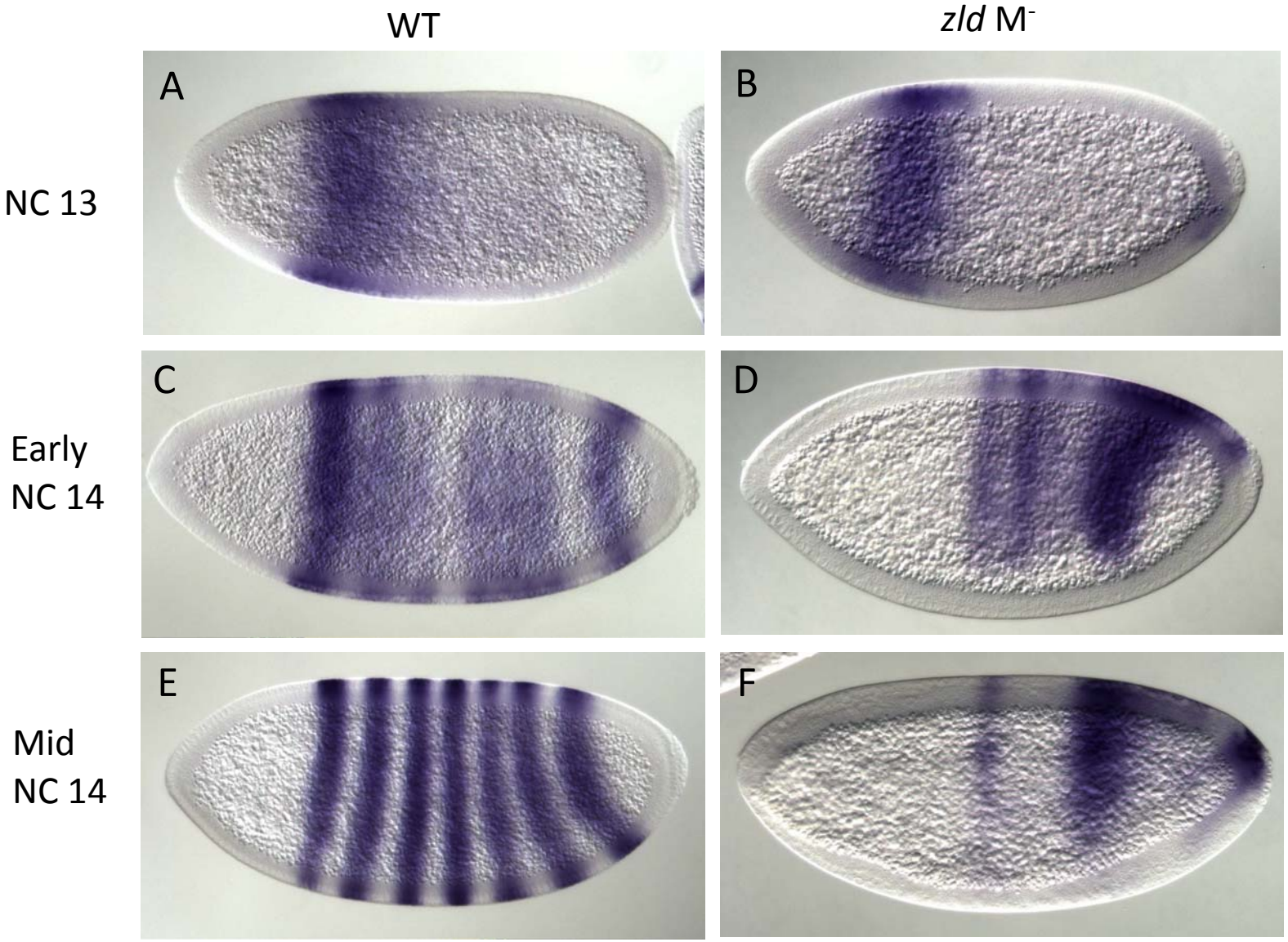
WT
zld M-
A
B
NC 13
C
D
Early
NC 14
E
F
Mid
NC 14

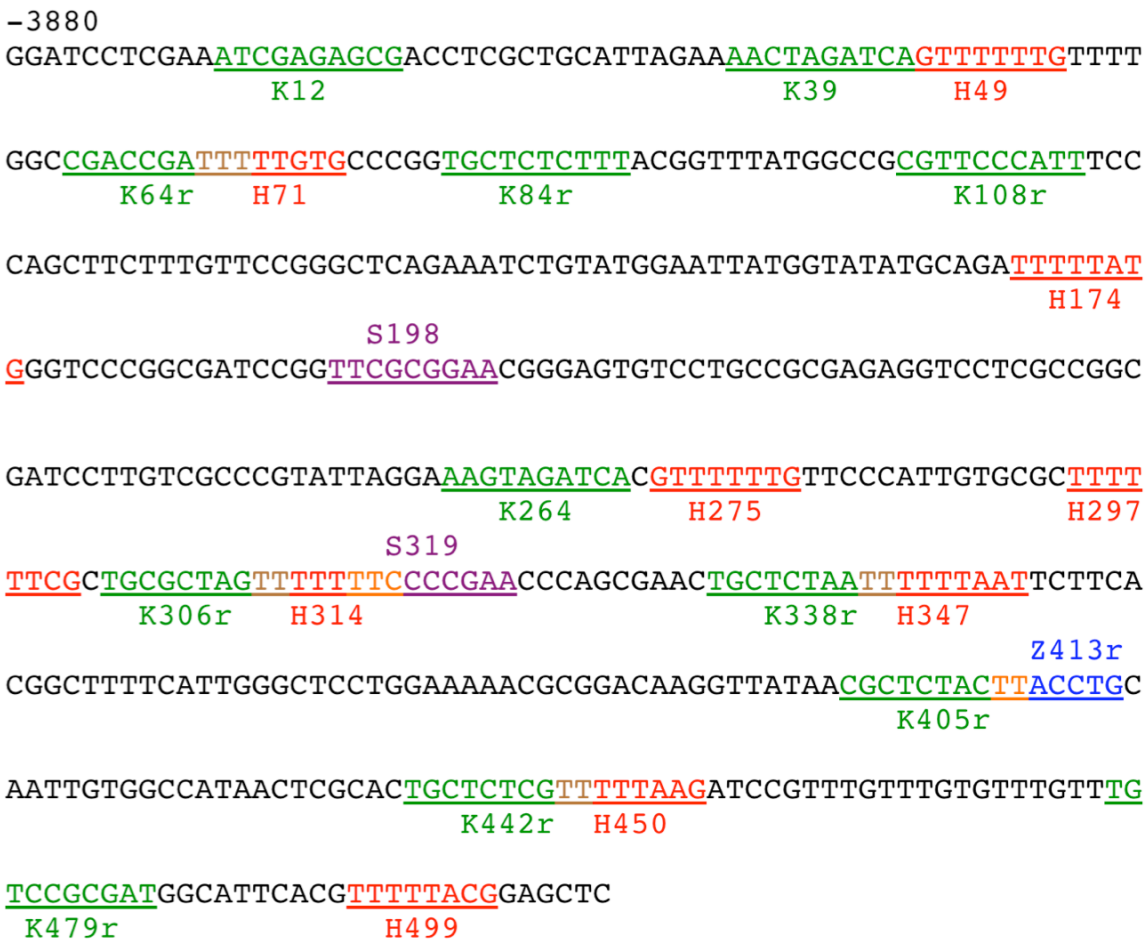

Legend:

Purple: STAT
Blue: Zelda
Green: Knirps
Red: Hunchback
Brown: overlap between repressors
Orange: overlap between activators and repressors

Table S1. Probes and primers

Name	Sequence	Binding	Position (nt)
Zelda gel-shift probe sequences for testing a binding site in the *eve* 3+7 enhancer (Fig. 2A)*			
Wild type	AACGCTCTACTTACCTGCAATT	Yes	403-424
Mutant	AACGCTCACTAGTAGTGCAATT	No	
Primers for PCR amplification of *eve* 2 sequences (Fig. 3F)†			
Fragment 1			
5′ oligo	GGCAGGAGCGAGGTATCCTTCCTG	Yes	–23-129
3′ oligo	CTGCAATTGACTAATAATCTCGCTG		
Fragment 2			
5′ oligo	GTTAATCCGTTTGCCATCAGCGAG	Yes	88-250
3′ oligo	CCCTCGATTCCGTCTAAATGAAAG		
Fragment 3			
5′ oligo	TTTAGACGGAATCGAGGGACCCTG	Yes	233-382
3′ oligo	GGATTCCAAGTCAAGCCCTTGGC		
Fragment 4			
5′ oligo	GCCAAGGGCTTGACTTGGAATCC	Yes	360-513
3′ oligo	CCGTTAATTGCGTTGCCTGGACC		
Probe sequences for testing Zelda binding to the *eve* 2 enhancer (Fig. 3G,H)‡			
P32	TAGCCAAGGGCTTGACTTGGA	No	358-378
P33	CTTGGAATCCAATCCCGATCC	No	373-393
P34	CGATCCCTAGCCCGATCCCAA	No	388-408
P35	TCCCAATCCCAATCCCAATCC	No	403-423
P36	CAATCCCTTGTCCTTTTCATT	No	418-438
P37	TTCATTAGAAAGTCATAAAAA	No	433-453
P38	TAAAAACACATAATAATGATG	No	448-468
P39	ATGATGTCGAAGGGATTAGGG	No	463-483
P40	TTAGGGGCGCGCAGGTCCAGG	No	478-498
P41	TCCAGGCAACGCAATTAACGG	Yes	493-513
P42	GCGCAGGTCCAGGCAACGCAAT	Yes	486-507
P43	GGCAGGAGCGAGGTATCCTTCC	Yes	–23 to –2
P44	CTTCCTGGTTACCCGGTACTGCAT	Weak	–6-18
P45	CGAAAAGCTGGCCTGGTTTCTCGC	Yes	52-75
P46	CGTGTTAATCCGTTTGCCATCA	No	85-106
P47	GTCGCAGTTTGGTAACACGCTG	No	198-219
P48	CTTTCATTTAGACGGAATCGAGGG	No	227-250
P49	CAGGGCATTCCGCCGATCTAGC	No	292-313
Knirps gel-shift probe sequences for testing binding sites in the *eve* 3+7 enhancer (Fig. 4A, Fig. 5)§			
P1	GACACAAGGATCCTCGAAATC	No	–7-14
P2	CTCGAAATCGAGAGCGACCTC	Yes	6-26
P2 M1	CTCGAAGTCGATAGAGACCTC	No	
P3	TGCATTAGAAAACTAGATCAG	Yes	29-49
P3 M1	TGCATTAGCTAGCTAGATCAG	No	
P3 M2	TGCATTAGAAGACTAAATTAG	No	
P3 M3	TGCATTAGAAAACTAAATTAG	Weak	
P3 M4	TGCATTAGAAAACTAAATCAG	Yes	
P3 M5	TGCATTAGAAAACTAGATTAG	Yes	
P4	TCAGTTTTTTGTTTTGGCCGACCGATTTTTGTG	Yes	46-78
P4 M1	TCAGTTTTTTGTTTTGGCCTACAGATTCTTGTG	Yes	
P4 M2	TCAGTTTTTTGTTTTAGCTTACAGATTTTTGTG	Yes	
P5	GTGCCCGGTGCTCTCTTTACG	Yes	76-96
P5 M1	GTGCCCGGTACTATCTTCACG	No	
P5 M2	GTGCCCGGTACTATCTTTACG	No	
P6	TATGGCCGCGTTCCCATTTCC	Yes	100-120
P6 M1	TATGGCCGCCTAGCCATTTCC	No	
P6 M2	TATGGCCGCATTACCATCTCC	No	
P7	AGCTTCTTTGTTCCGGGCTCA	No	122-142
P8	CAGAAATCTGTATGGAATTATG	No	141-162
P9	TTATGGTATATGCAGATTTTTATGG	No	158-182
P10	TTATGGGTCCCGGCGATCCGGTTC	No	177-200
P11	GGTTCGCGGAACGGGAGTGTC	No	196-216
P12	GTGTCCTGCCGCGAGAGGTCCTCGC	No	212-236
P13	CTCGCCGGCGATCCTTGTCGC	No	232-252
P14	TTGTCGCCCGTATTAGGA	Weak	246-263
P14 M1	TTGTCACCAGTATTAGGA	No	
P15	CGTATTAGGAAAGTAGATCAC	Yes	254-274
P15 M1	CGTATTAGCTAGGTAGATCAC	No	
P15 M2	CGTATTAGGAGAGTATATTAC	No	

P16	GTAGATCACGTTTTTTGTTC	No	266-285
P17	ACGTTTTTTGTTCCCATTGTG	No	273-293
P18	ATTGTGCGCTTTTTTCGCT	No	288-306
P19	TTTTTCGCTGCGCTAGTTTTT	Yes	298-318
P19 M1	TTTTTCGCTACGATAGTCTTT	No	
P19 M2	TTTTTCGCTACGATAGTTTTT	No	
P20	GCTAGTTTTTTTCCCCGAACC	No	309-329
P21	GAACCCAGCGAACTGCTCTAATT	Yes	325-347
P21 M1	GAACCCAGCGAACTACTATAATC	No	
P21 M2	GAACCCAGCGAACTACTATAATT	No	
P22	TAATTTTTTAATTCTTCACGGCTTTT	Weak	343-368
P23	TTTTCATTGGGCTCCTGGAAAAAACG	Weak	365-389
P24	AAACGCGGACAAGGTTATAACGC	No	385-407
P25	AACGCTCTACTTACCTGCAATT	Yes	403-424
P25 M1	AACACTTTACTTACCTGCAATT	No	
P25 M2	AACGCCGGTCTTACCTGCAATT	No	
P26	AATTGTGGCCATAACTCGCACTGC	No	421-444
P27	ACTGCTCTCGTTTTTAAGAT	Yes	440-459
P27 M1	ACTGCTCTCCTAGTTAAGAT	No	
P27 M2	ACTACTATCGTCTTTAAGAT	No	
P27 M3	ACTACTATCGTTTTTAAGAT	No	
P28	GTTTTTAAGATCCGTTTGT	No	449-467
P29	TTTGTTTGTGTTTGTTTGTCCGCGATGGCAT	Yes	463-493
P29 M1	TTTGTTTGTGTTTGTTTATCAGCGACGGCAT	Yes	
P30	GGCATTCACGTTTTTACGAGC	No	489-509
P31	ACGAGCTCGTTCCTTCGGGTCCA	No	504-526

*The TAGteam sequence is underlined. Numbers refer to nucleotide position with respect to the minimal *eve* 3+7 enhancer tested in vivo and reported in Fig. S4.

†Numbers refer to the nucleotide position with respect to the minimal *eve* 2 enhancer tested in vivo, which spans from the *Bst*EII site on the 5′ side to the *Bss*HII site on the 3′ side (i.e. nucleotides 1-489).

‡The putative Zelda binding sites are underlined. Numbers are as above.

§Knirps binding sites are in blue. Tested mutations are in red. Numbers refer to the nucleotide position with respect to the minimal *eve* 3+7 enhancer tested in vivo and reported in Fig. S4.